

---

# FIT: Parameter Efficient Few-shot Transfer Learning for Personalized and Federated Image Classification

---

**Aliaksandra Shysheya\***  
University of Cambridge  
as2975@cam.ac.uk

**John Bronskill\***  
University of Cambridge  
jfb54@cam.ac.uk

**Massimiliano Patacchiola**  
University of Cambridge  
mp2008@cam.ac.uk

**Sebastian Nowozin**  
Microsoft Research  
senowoz@microsoft.com

**Richard E. Turner**  
University of Cambridge  
ret26@cam.ac.uk

## Abstract

Modern deep learning systems are increasingly deployed in situations such as personalization and federated learning where it is necessary to support i) learning on small amounts of data, and ii) communication efficient distributed training protocols. In this work we develop FiLM Transfer (FiT) which fulfills these requirements in the image classification setting. FiT uses an automatically configured Naive Bayes classifier on top of a fixed backbone that has been pretrained on large image datasets. Parameter efficient FiLM layers are used to modulate the backbone, shaping the representation for the downstream task. The network is trained via an episodic fine-tuning protocol. The approach is parameter efficient which is key for enabling few-shot learning, inexpensive model updates for personalization, and communication efficient federated learning. We experiment with FiT on a wide range of downstream datasets and show that it achieves better classification accuracy than the state-of-the-art Big Transfer (BiT) algorithm at low-shot and on the challenging VTAB-1k benchmark, with fewer than 1% of the updateable parameters. Finally, we demonstrate the parameter efficiency of FiT in distributed low-shot applications including model personalization and federated learning where model update size is an important performance metric.

## 1 Introduction

With the success of the commercial application of deep learning in many fields such as computer vision [1], natural language processing [2], speech recognition [3], and language translation [4], an increasing number of models are being trained on central servers and then deployed on remote devices, often to personalize a model to a specific user’s needs. Personalization requires models that can be updated inexpensively by minimizing the number of parameters that need to be stored and/or transmitted and frequently calls for few-shot learning methods as the amount of training data from an individual user may be small [5]. At the same time, for privacy, security, and performance reasons, it can be advantageous to use federated learning where a model is trained on an array of remote devices, each with different data, and share gradient or parameter updates instead of training data with a central server [6]. In the federated learning setting, in order to minimize communication cost with the server, it is beneficial to have models with a small number of parameters that need to be updated for each training round conducted by remote clients. The amount of training data available to the clients is often small, again necessitating few-shot learning approaches.

---

\* Authors contributed equally

Few-shot learning approaches fall broadly into two camps – meta-learning [7] and transfer learning (fine-tuning) [8]. It is useful to characterise these approaches in terms of shared and updateable parameters. Shared parameters do not change as the model is retrained or updated, while updateable parameters are those that are either recomputed or learned as the model is updated or retrained. From a statistical perspective, shared parameters capture similarities between datasets, while updateable parameters efficiently capture the differences. In general, meta-learning approaches [7] to few-shot learning are trained in a multi-task manner and as a result share a large number of parameters and only update a small subset when adapting to a new task [9]. While meta-learners can achieve good accuracy on datasets that are similar to what they are meta-trained on, their accuracy suffers when tested on datasets that are significantly different [10]. Transfer learning algorithms can often outperform meta-learners, especially on diverse datasets and even at low-shot [10, 11]. While some transfer learning algorithms are able to minimize the number of updateable parameters by only fine-tuning the final or a small subset of layers, the state of the art Big Transfer (BiT) [10, 12] algorithm requires every parameter in a large network to be updated.

In this work, we focus on designing deep learning network architectures and associated training protocols that allow image classification models to be updated with only a small subset of the total model parameters, without sacrificing prediction performance when there is only a small number of training examples available. This leads to reduced storage and transmission costs for updating personalized models on remote devices [5], distributed training in federated learning [6], and efficient ensemble realization [13], among other applications. To realize our goal of small model updates, we pursue a transfer learning approach that takes advantage of image classification backbones that have been pretrained on large upstream datasets [12]. We freeze the backbone parameters such that they are shared when fine-tuning on a downstream dataset. Parameter efficient FiLM [14] adapter layers are used to modulate the backbone, shaping the representation for the downstream task. For a ResNet50 [15], the FiLM layer parameter count is less than 0.05% of the overall model size, yet allows expressive adaptation. The last, novel piece of the proposed system is the use of an automatically configured Naive Bayes final layer classifier which outperforms the usual linear layer head. The system is trained end-to-end with an episodic fine-tuning protocol. We call this approach FiLM Transfer or FiT. We experiment with FiT on a wide range of downstream datasets and show that it achieves better classification accuracy at low-shot with two orders of magnitude fewer updateable parameters when compared to BiT [12] and competitive accuracy when more data is available. We also demonstrate the benefits of FiT on a low-shot real-world model personalization application and in a demanding few-shot federated learning scenario. Our contributions:

- A parameter and data efficient network architecture for low-shot transfer learning consisting of an automatically configured Naive Bayes final layer classifier and parameter efficient FiLM layers that are used to adapt a fixed, pretrained backbone to a downstream dataset;
- A meta-learning inspired episodic training protocol for low-shot fine-tuning requiring no data augmentation, no regularization, and a minimal set of hyper-parameters;
- Superior classification accuracy at low-shot on standard downstream datasets and on the challenging VTAB-1k benchmark while using  $\approx 1\%$  of the updateable parameters when compared to the leading transfer learning method BiT;
- Demonstration of superior parameter efficiency without sacrificing classification accuracy in distributed low-shot applications including model personalization and federated learning where model update size is important performance metric.

## 2 FiLM Transfer (FiT)

In this section we detail the FiT algorithm focusing on the few-shot image classification scenario.

**Preliminaries** We denote input images  $\mathbf{x} \in \mathbb{R}^{ch \times W \times H}$  where  $W$  is the width,  $H$  the height,  $ch$  the number of channels and image labels  $y \in \{1, \dots, C\}$  where  $C$  is the number of image classes indexed by  $c$ . Assume that we have access to a model  $f(\mathbf{x}) = h_\phi(b_\theta(\mathbf{x}))$  that outputs  $p(y = c | \mathbf{x})$  for  $c = 1, \dots, C$  and is comprised of a feature extractor backbone  $b_\theta(\mathbf{x}) \in \mathbb{R}^{d_b}$  with parameters  $\theta$  that has been pretrained on a large upstream dataset such as Imagenet [16] where  $d_b$  is the output feature dimension and a final layer classifier or head  $h_\phi(\cdot) \in \mathbb{R}^C$  with weights  $\phi$ . Let  $\mathcal{D} = \{(\mathbf{x}_n, y_n)\}_{n=1}^N$  be the downstream dataset that we wish to fine-tune the model  $f$  to.

**FiT Backbone** For the backbone, we freeze the parameters  $\theta$  to the values learned during upstream pretraining and add Feature-wise Linear Modulation (FiLM) [14] layers with parameters  $\psi$  at strategic points within  $b_\theta$ . A FiLM layer scales and shifts the activations  $\mathbf{a}_{ij}$  arising from the  $j^{\text{th}}$  channel of a convolutional layer in the  $i^{\text{th}}$  block of the backbone as  $\text{FiLM}(\mathbf{a}_{ij}, \gamma_{ij}, \beta_{ij}) = \gamma_{ij}\mathbf{a}_{ij} + \beta_{ij}$ , where  $\gamma_{ij}$  and  $\beta_{ij}$  are scalars. The set of FiLM parameters  $\psi = \{\gamma_{ij}, \beta_{ij}\}$  are learned during fine-tuning. We add FiLM layers following the middle  $3 \times 3$  convolutional layer in each ResNetV2 [17] block and also one at the end of the backbone prior to the head. Fig. A.1a illustrates a FiLM layer operating on a convolutional layer, and Fig. A.1b illustrates how a FiLM layer can be added to a ResNetV2 network block. FiLM layers can be similarly added to EfficientNet based backbones. A key advantage of FiLM layers is that they enable expressive feature adaptation while adding only a small number of parameters [14]. For example, in a ResNet50 with a FiLM layer in every block, the set of FiLM parameters  $\psi$  account for only 11648 parameters which is fewer than 0.05% of the parameters in  $b_\theta$ . We show in Section 4 that FiLM layers allow the model to adapt to a broad class of datasets.

**FiT Head** For the head, we use a Gaussian Naive Bayes classifier which can be automatically configured directly from data. If the data is normally distributed, Naive Bayes is generally more effective than logistic regression [18, 19], and especially so in the small data setting [20]. Also, when compared to the usual linear layer head, Naive Bayes has fewer free parameters to learn and in Section 4 we show that it yields superior results. The probability of classifying a test point  $\mathbf{x}^*$  is:

$$p(y^* = c | b_{\theta, \psi}(\mathbf{x}^*), \boldsymbol{\pi}, \boldsymbol{\mu}, \boldsymbol{\Sigma}) = \frac{\pi_c \mathcal{N}(b_{\theta, \psi}(\mathbf{x}^*) | \mu_c, \Sigma_c)}{\sum_{c'} \pi_{c'} \mathcal{N}(b_{\theta, \psi}(\mathbf{x}^*) | \mu_{c'}, \Sigma_{c'})} \quad (1)$$

where  $\pi_c = \frac{N_c}{N}$ ,  $\mu_c = \frac{1}{N_c} \sum_{i=1}^{N_c} b_{\theta, \psi}(\mathbf{x}_i)$ ,  $\Sigma_c = \frac{1}{N_c} \sum_{i=1}^{N_c} (b_{\theta, \psi}(\mathbf{x}_i) - \mu_c)(b_{\theta, \psi}(\mathbf{x}_i) - \mu_c)^T$

are the maximum likelihood estimates,  $N_c$  is the number of examples of class  $c$  in  $\mathcal{D}$ , and  $\mathcal{N}(z | \mu, \Sigma)$  is a multivariate Gaussian over  $z$  with mean  $\mu$  and covariance  $\Sigma$ .

Estimating the mean  $\mu_c$  for each class  $c$  is straightforward and incurs a total storage cost of  $Cd_b$ . However, estimating the covariance  $\Sigma_c$  for each class  $c$  is challenging when the number of examples per class  $N_c$  is small and the embedding dimension of the backbone  $b_d$  is large. In addition, the storage cost for the covariance matrices may be prohibitively high if  $d_b$  is large. In this work, we use three different approximations to the covariance in place of  $\Sigma_c$  in Eq. (1):

- **Quadratic Discriminant Analysis (QDA)** [21, 22]:  $\Sigma_{\text{QDA}} = e_1 \Sigma_{\text{class}} + e_2 \Sigma_{\text{task}} + e_3 I$
- **Linear Discriminant Analysis (LDA)** [21, 22]:  $\Sigma_{\text{LDA}} = e_2 \Sigma_{\text{task}} + e_3 I$
- **ProtoNets** [23]:  $\Sigma_{\text{PN}} = I$ ; Or equivalently, there is no covariance and the class representation is parameterized only by  $\mu_c$  and the classifier logits are formed by computing the squared Euclidean distance between the feature representation of a test point  $b_{\theta, \psi}(\mathbf{x}^*)$  and each of the class means.

In the above,  $\Sigma_{\text{class}}$  is the computed covariance of the examples in class  $c$  in  $\mathcal{D}$ ,  $\Sigma_{\text{task}}$  is the computed covariance of all the examples in  $\mathcal{D}$  assuming they arise from a single Gaussian with a single mean,  $\mathbf{e} = \{e_1, e_2, e_3\}$  are weights learned during training, and the identity matrix  $I$  is used as a regularizer. The primary difference between QDA and LDA is that QDA computes and stores a covariance matrix for each class in the dataset, while LDA shares a single covariance matrix across all classes. The number of model shared and updateable parameters for the three FiT variants as well as the BiT algorithm are detailed in Table A.1. Using the BiT-M-R50x1 [12] backbone on a 10-way classification task, BiT shares no parameters and all 23.52M parameters are updateable. FiT shares the 25.50M backbone parameters and FiT-QDA, FiT-LDA, and FiT-ProtoNets have 21.01M, 32,140, and 32,128 updateable parameters, respectively. The parameters  $\theta$  are known and fixed from pretraining, but we must learn the FiLM parameters  $\psi$  and the covariance weights  $\mathbf{e}$  as outlined in the next section.

**FiT Training** We learn  $\psi$  and  $\mathbf{e}$  via fine-tuning, but employ an approach often used in meta-learning referred to as *episodic training* [24] to form the training batches. Note we require ‘training’ data to compute  $\boldsymbol{\pi}, \boldsymbol{\mu}, \boldsymbol{\Sigma}$  to configure the head, and a ‘test’ set to optimize  $\psi$  and  $\mathbf{e}$  via gradient ascent. Thus, from the downstream dataset  $\mathcal{D}$ , we derive two sets –  $\mathcal{D}_{\text{train}}$  and  $\mathcal{D}_{\text{test}}$ . If  $\mathcal{D}$  is sufficiently large ( $|\mathcal{D}| \approx 1000$ ), we set  $\mathcal{D}_{\text{train}} = \mathcal{D}_{\text{test}} = \mathcal{D}$ . Otherwise, in the few-shot scenario, we randomly split  $\mathcal{D}$  into  $\mathcal{D}_{\text{train}}$  and  $\mathcal{D}_{\text{test}}$  such that the number of examples or *shots* in each class  $c$  are roughly equal in both partitions and that there is at least one example of each class in both. Refer to Algorithm A.1 for details. For each training iteration, we sample a task  $\tau$  consisting of a *support* set  $\mathcal{D}_\tau^s$  drawn

from  $\mathcal{D}_{train}$  with  $S_\tau$  examples and a *query*  $\mathcal{D}_Q^\tau$  set drawn from  $\mathcal{D}_{test}$  with  $Q_\tau$  examples. First,  $\mathcal{D}_S^\tau$  is formed by randomly choosing a subset of classes selected from the range of available classes in  $\mathcal{D}_{train}$ . Second, the number of shots to use for each selected class is randomly selected from the range of available examples in each class of  $\mathcal{D}_{train}$  with the goal of keeping the examples per class as equal as possible. Third,  $\mathcal{D}_Q^\tau$  is formed by using the classes selected for  $\mathcal{D}_S^\tau$  and all available examples from  $\mathcal{D}_{test}$  in those classes up to a limit of 2000 examples. Refer to Algorithm A.2 for details. Episodic task sampling is crucial to achieving the best classification accuracy. If all of  $\mathcal{D}_{train}$  and  $\mathcal{D}_{test}$  are used for every iteration, overfitting occurs, limiting accuracy (see Table A.3 and Table A.4). The support set  $\mathcal{D}_S^\tau$  is then used to compute  $\boldsymbol{\pi}$ ,  $\boldsymbol{\mu}$ , and  $\boldsymbol{\Sigma}$  and we then use  $\mathcal{D}_Q$  to train  $\boldsymbol{\psi}$  and  $\boldsymbol{e}$  with maximum likelihood. We optimize the following objective:

$$\hat{\mathcal{L}}(\boldsymbol{\psi}, \boldsymbol{e}) = \sum_{\tau=1}^T \sum_{q=1}^{Q_\tau} \log p(y_q^* | h_e(b_{\theta, \boldsymbol{\psi}}(\boldsymbol{x}_q^*)), \boldsymbol{\pi}(\mathcal{D}_S^\tau), \boldsymbol{\mu}(\mathcal{D}_S^\tau), \boldsymbol{\Sigma}(\mathcal{D}_S^\tau)). \quad (2)$$

FiT training hyperparameters include a learning rate,  $|\mathcal{D}_S^\tau|$ , and the number of training iterations. For the transfer learning experiments in Section 4 these are set to constant values across all datasets and do not need to be tuned based on a validation set. We do not augment the training data, even in the 1-shot case. When there is only one shot per class, we leave the FiLM layer parameters at their initial value of  $\gamma = 1$  and  $\beta = 0$  and predict as described in the next paragraph. In Section 4 we show this can yield results that surpass those when augmentation and training steps are taken on the 1-shot data.

**FiT Prediction** Once the FiLM parameters  $\boldsymbol{\psi}$  and covariance weights  $\boldsymbol{e}$  have been learned, we use  $\mathcal{D}$  for the support set to compute  $\pi_c$ ,  $\mu_c$ , and  $\Sigma_c$  for each class  $c$  and then Eq. (1) can be used to make a prediction for any unseen test input.

### 3 Related Work

We take inspiration from residual adapters [25, 26] where parameter efficient adapters are inserted into a ResNet with frozen pretrained weights. The adapter parameters and the final layer linear classifier are then learned via fine-tuning. FiT differs from residual adapters by focusing on the few-shot scenario, and using FiLM layers that have fewer parameters than a residual adapter, a Naive Bayes head, and an episodic training protocol. CNAPs [9] also uses a frozen, pretrained backbone with FiLM layers added. The FiLM parameters and a linear head are generated by meta-trained hypernetworks. Simple CNAPs [27] improves on CNAPs by using a Mahalanobis distance based classifier that uses a blend of class specific and task specific covariance matrices. FiT-LDA greatly improves over Simple CNAPs [28] in terms of classification accuracy and updateable parameters on the VTAB-1k benchmark as a result of using fine-tuning instead of amortization networks and using a single dataset specific covariance matrix as opposed to class specific one.

FLUTE [29] during multi-task training jointly learns backbone parameters along with a set of dataset specific FiLM layer parameters. When asked to classify a novel input at test-time, the backbone parameters are frozen and a Blender network generates initial values for the FiLM parameters using a combination of those that it has learned in the training phase and the test task. The initial FiLM parameters are then improved via fine-tuning through a nearest centroid final layer classifier. FiT differs from FLUTE in that (i) there is no initial multi-task learning phase; (ii) more fine-tuning iterations; and (iii) the use of a Naive Bayes head. The work of Mudrakarta et al. [30] has the same aim as this work. Instead of fine-tuning FiLM layers that are added to a pretrained network, batch normalization weights are tuned. While this work is similar in spirit, unlike FiT, it does not focus on the few-shot regime, employs a linear head, and uses a more conventional fine-tuning protocol.

### 4 Experiments

In this section, we evaluate the classification accuracy and updateable parameter efficiency of FiT in a series of challenging benchmarks and application scenarios. First, we compare different variations of FiT to Big Transfer (BiT) [12], a state-of-the-art transfer learning algorithm, on several standard downstream datasets in the few-shot regime. Second, we evaluate FiT against BiT on the challenging VTAB-1k benchmark [31], where BiT has been shown to outperform all meta-learners [10, 28]. Third, we show how FiT can be used in a personalization scenario on the ORBIT [5] dataset,

where a smaller updateable model is an important evaluation metric. Finally, we apply FiT to a few-shot federated learning scenario where minimizing the number of parameter updates and their size is a key requirement. In addition, we introduce a metric *Relative Model Update Size* or RMUS, which is the ratio of the number of updateable parameters in one model to another. Training and evaluation details are in Appendix A.5. Source code for experiments can be found at: <https://github.com/cambridge-mlg/fit>.

#### 4.1 Few-shot Results

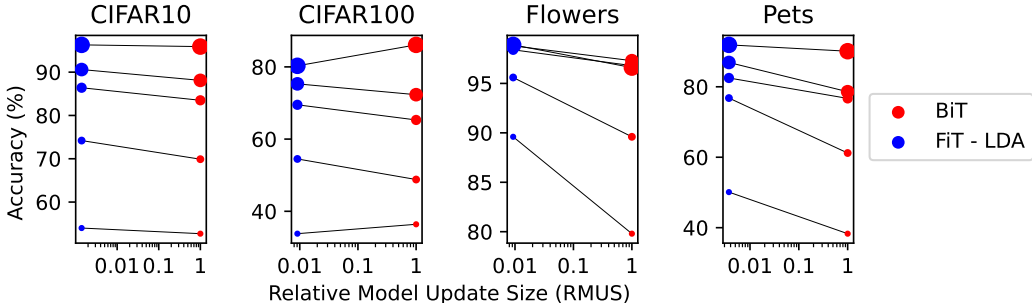


Figure 1: **FiT-LDA outperforms BiT at low-shot.** Classification accuracy as a function of Relative Model Update Size (RMUS – lower is better) and shots per class for FiT-LDA and BiT on four downstream datasets. Classification accuracy is on the vertical axis and is the average of 3 runs with different data sampling seeds. RMUS is relative to the number of updateable parameters for BiT and uses a base 10 log scale. The dot size from smallest to largest indicates the number of shots per class - 1, 2, 5, 10, and All. A tabular version that includes results for additional variants is in Table A.2.

Fig. 1 shows the classification accuracy as a function of RMUS for FiT-LDA and BiT on four downstream datasets (CIFAR10, CIFAR100 [32], Flowers [33], and Pets [34]) that were used to evaluate the performance of BiT [12]. Table A.2 contains complete tabular results with additional variants of FiT and BiT. All methods use the BiT-M-R50x1 [12] backbone that has been pretrained on the ImageNet-21K [16] dataset. The key observations from Fig. 1 are:

- For  $\leq 10$  shots (except 1-shot on CIFAR100), FiT-LDA outperforms BiT, often by a large margin.
- On 3 out of 4 datasets, FiT-LDA outperforms BiT even when all of  $\mathcal{D}$  is used for fine-tuning.
- FiT-LDA outperforms BiT despite BiT having more than 100 times as many updateable parameters.
- To avoid overfitting when  $\mathcal{D}$  is small, Table A.3 indicates that it is better to split  $\mathcal{D}$  into two disjoint partitions  $\mathcal{D}_{train}$  and  $\mathcal{D}_{test}$  and that  $\mathcal{D}_S^r$  and  $\mathcal{D}_Q^r$  should be randomly sub-sampled as opposed to using all of the data in each training iteration.

We also evaluate BiT-FiLM, a variant of BiT that uses the same training protocol as the standard version of BiT, but the backbone weights  $\theta$  are frozen and FiLM layers are added in the same manner as FiT. The FiLM parameters  $\psi$  and the linear head weights  $\phi$  are learned during training. The results are shown in Table A.2 and the key observations are:

- In general, at low-shot, the standard version of BiT outperforms BiT-FiLM. However, as the shot increases, especially when training on all of  $\mathcal{D}$ , BiT-FiLM is equal in classification accuracy.
- The above implies that FiLM layers have sufficient capacity to accurately fine-tune to downstream datasets, but the FiT head and training protocol are needed to achieve superior results.
- While the accuracy of FiT-QDA and FiT-LDA is similar, the storage requirements for a covariance matrix for each class makes QDA impractical if model update size is an important consideration.
- The accuracy of FiT-ProtoNets is slightly lower than FiT-LDA, but often better than BiT, despite BiT having more than 100 times as many updateable parameters.

The datasets used in this section were similar in content to the dataset used for pretraining and the performance of FiT-QDA and FiT-LDA was similar, indicating that the covariance per class was not that useful for these datasets. In the next section, we test on a wider variety of datasets, many of which differ greatly from the upstream data.

## 4.2 VTAB-1k Results

The VTAB-1k benchmark [31] is a low to medium-shot transfer learning benchmark that consists of 19 datasets grouped into three distinct categories (natural, specialized, and structured). From each dataset, 1000 examples are drawn at random from the training split to use for the downstream dataset  $\mathcal{D}$ . After fine-tuning, the entire test split is used to evaluate classification performance. Table 1 shows the classification accuracy of the three variants of FiT and BiT using the BiT-M-R50x1 backbone for all variants. The key observations from our results are:

- Both FiT-QDA and FiT-LDA outperform BiT on VTAB-1k.
- The FiT-QDA variant has the best overall performance, showing that the class covariance is important to achieve superior results on datasets that differ from those used in upstream pretraining (e.g. the structured category of datasets). However, the updateable parameter cost is high.
- FiT-LDA utilizes two orders of magnitude fewer updateable parameters compared to BiT, making it the preferred approach.
- Table A.4 indicates that it is best to use all of  $\mathcal{D}$  for each of  $\mathcal{D}_{train}$  and  $\mathcal{D}_{test}$  (i.e. no split) and that  $\mathcal{D}_S^\tau$  and  $\mathcal{D}_Q^\tau$  should be randomly sub-sampled as opposed to using all of the data in each iteration.

Table 1: **FiT outperforms BiT on VTAB-1k.** Classification accuracy and Relative Model Update Size (RMUS) for all three variants of FiT and BiT on the VTAB-1k benchmark. The backbone is BiT-M-R50x1. Accuracy figures are percentages and the  $\pm$  sign indicates the 95% confidence interval over 3 runs. Bold type indicates the highest scores (within the confidence interval).

Dataset	BiT			FiLM Transfer (FiT)					
	C	Accuracy $\uparrow$	RMUS $\downarrow$	QDA		LDA		ProtoNets	
				Accuracy $\uparrow$	RMUS $\downarrow$	Accuracy $\uparrow$	RMUS $\downarrow$	Accuracy $\uparrow$	RMUS $\downarrow$
Caltech101 [35]	102	88.0 $\pm$ 0.2	1.0	<b>90.3<math>\pm</math>0.8</b>	9.04	<b>90.4<math>\pm</math>0.8</b>	<b>0.0093</b>	<b>89.6<math>\pm</math>0.2</b>	<b>0.0093</b>
CIFAR100 [32]	100	70.1 $\pm$ 0.1	1.0	<b>74.1<math>\pm</math>0.1</b>	8.86	<b>74.2<math>\pm</math>0.5</b>	<b>0.0091</b>	<b>73.9<math>\pm</math>0.3</b>	<b>0.0091</b>
Flowers102 [33]	102	98.6 $\pm$ 0.0	1.0	<b>99.1<math>\pm</math>0.1</b>	9.04	<b>99.0<math>\pm</math>0.1</b>	<b>0.0093</b>	98.6 $\pm$ 0.0	<b>0.0093</b>
Pets [34]	37	88.4 $\pm$ 0.2	1.0	<b>91.0<math>\pm</math>0.3</b>	3.30	90.5 $\pm$ 0.0	<b>0.0037</b>	<b>90.8<math>\pm</math>0.2</b>	<b>0.0037</b>
Sun397 [36]	397	48.0 $\pm$ 0.1	1.0	<b>51.1<math>\pm</math>0.7</b>	34.29	<b>51.6<math>\pm</math>0.5</b>	<b>0.0339</b>	<b>51.5<math>\pm</math>1.4</b>	<b>0.0339</b>
SVHN [37]	10	73.0 $\pm$ 0.2	1.0	<b>75.1<math>\pm</math>1.3</b>	0.89	<b>74.2<math>\pm</math>0.9</b>	<b>0.0014</b>	50.1 $\pm$ 2.2	<b>0.0014</b>
DTD [38]	47	<b>72.7<math>\pm</math>0.3</b>	1.0	70.9 $\pm$ 0.1	4.18	70.9 $\pm$ 0.1	<b>0.0046</b>	68.2 $\pm$ 1.1	<b>0.0046</b>
EuroSAT [39]	10	95.3 $\pm$ 0.1	1.0	<b>95.6<math>\pm</math>0.1</b>	0.89	95.1 $\pm$ 0.1	<b>0.0014</b>	93.8 $\pm$ 0.1	<b>0.0014</b>
Resisc45 [40]	45	<b>85.9<math>\pm</math>0.0</b>	1.0	82.6 $\pm$ 0.1	4.01	82.5 $\pm$ 0.2	<b>0.0044</b>	77.0 $\pm$ 0.0	<b>0.0044</b>
Patch Camelyon [41]	2	69.3 $\pm$ 0.8	1.0	<b>80.7<math>\pm</math>1.2</b>	0.18	<b>82.5<math>\pm</math>0.7</b>	<b>0.0007</b>	79.9 $\pm$ 0.2	<b>0.0007</b>
Retinopathy [42]	5	<b>77.2<math>\pm</math>0.6</b>	1.0	70.4 $\pm$ 0.1	0.45	66.2 $\pm$ 0.5	<b>0.0009</b>	57.9 $\pm$ 0.3	<b>0.0009</b>
CLEVR-count [43]	8	54.6 $\pm$ 7.1	1.0	87.1 $\pm$ 0.3	0.71	85.6 $\pm$ 0.9	<b>0.0012</b>	<b>88.7<math>\pm</math>0.3</b>	<b>0.0012</b>
CLEVR-dist [43]	6	47.9 $\pm$ 0.8	1.0	<b>58.1<math>\pm</math>0.8</b>	0.54	56.1 $\pm$ 0.8	<b>0.0010</b>	<b>58.3<math>\pm</math>0.6</b>	<b>0.0010</b>
dSprites-loc [44]	16	<b>91.6<math>\pm</math>1.1</b>	1.0	77.1 $\pm$ 2.0	1.43	74.8 $\pm$ 1.4	<b>0.0019</b>	68.6 $\pm$ 2.4	<b>0.0019</b>
dSprites-ori [44]	16	<b>65.9<math>\pm</math>0.3</b>	1.0	56.7 $\pm$ 0.3	1.43	51.3 $\pm$ 0.7	<b>0.0019</b>	34.2 $\pm$ 0.8	<b>0.0019</b>
SmallNORB-azi [45]	18	<b>18.7<math>\pm</math>0.2</b>	1.0	<b>18.9<math>\pm</math>0.6</b>	1.61	16.2 $\pm$ 0.1	<b>0.0021</b>	13.5 $\pm$ 0.1	<b>0.0021</b>
SmallNORB-elev [45]	9	25.8 $\pm$ 0.9	1.0	<b>40.4<math>\pm</math>0.2</b>	0.80	37.0 $\pm$ 0.6	<b>0.0013</b>	35.0 $\pm$ 0.6	<b>0.0013</b>
DMLab [46]	6	<b>47.1<math>\pm</math>0.1</b>	1.0	43.8 $\pm$ 0.3	0.54	41.6 $\pm$ 0.6	<b>0.0010</b>	39.3 $\pm$ 0.3	<b>0.0010</b>
KITTI-dist [47]	4	<b>80.1<math>\pm</math>0.9</b>	1.0	77.5 $\pm$ 0.7	0.36	77.7 $\pm$ 0.8	<b>0.0008</b>	75.3 $\pm$ 0.2	<b>0.0008</b>
All		68.3		<b>70.6</b>		69.3		65.5	
Natural		77.0		<b>78.8</b>		78.7		74.7	
Specialized		81.9		<b>82.3</b>		81.5		77.1	
Structured		54.0		<b>57.5</b>		55.0		51.6	

## 4.3 Personalization

In our experiments, we use ORBIT [5], a real-world few-shot video dataset recorded by people who are blind/low-vision. A blind or vision-impaired user collects a series of short videos on their smartphone of objects that they would like to recognize. The collected videos and associated labels are then uploaded to a central service to train a personalized classification model for that user. Once trained, the personalized model is downloaded to the user’s smartphone. The initial model download would include all the model parameters, both shared and updateable. However, models with a smaller number of updateable parameters are preferred in order to save model storage space on the central server and in transmitting any updated models to a user. The goal is to take a backbone pretrained on ImageNet [48] or other large-scale dataset and construct a personalized model for a user using only their individual data. We follow the object recognition benchmark task proposed by the authors, which tests a personalized model on two different video types: *clean* where only a single object is present and *clutter* where that object appears within a realistic, multi-object scene.

Table 2: **FiT outperforms competitive methods on ORBIT.** Average accuracy (95% confidence interval) over 85 test tasks. Shared is the number of parameters shared among all users. Per User indicates the number of parameters stored for each user with  $C$  classes. Average is the mean number of individual user parameters over the ORBIT dataset.

MODEL	Clean Videos		Clutter Videos		Parameters		
	FRAME ACC $\uparrow$	VIDEO ACC $\uparrow$	FRAME ACC $\uparrow$	VIDEO ACC $\uparrow$	SHARED $\downarrow$	PER USER $\downarrow$	AVERAGE $\downarrow$
FineTuner [8]	<b>78.1 (2.0)</b>	85.9 (2.3)	<b>63.1 (1.8)</b>	66.9 (2.4)	<b>4.01M</b>	$(d_b + 1)C$	<b>0.01M</b>
Simple CNAPs [27]	73.1 (2.1)	80.7 (2.6)	61.6 (1.8)	67.1 (2.4)	5.67M	$\frac{d_b(d_b+3)}{2}C$	7.63M
ProtoNets [23]	71.6 (2.2)	78.9 (2.7)	63.0 (1.8)	67.3 (2.4)	<b>4.01M</b>	$d_b C$	<b>0.01M</b>
FiT-LDA	<b>81.8 (1.8)</b>	<b>90.6 (1.9)</b>	<b>65.7 (1.8)</b>	<b>70.7 (2.3)</b>	<b>4.01M</b>	$(d_b + 1)C +  \psi $	0.03M

In Table 2, we compare FiT-LDA to several competitive transfer learning and meta-learning methods. We use the LDA variant of FiT, as it achieves higher accuracy in comparison to the ProtoNets variant, while using far fewer updateable parameters than QDA. For transfer learning, we include FineTuner [8], which freezes the weights in the backbone and fine-tunes only the linear classifier head on an individual’s data. For meta-learning approaches, we include ProtoNets [23] and Simple CNAPs [27], which are meta-trained on Meta-Dataset [10]. Training and evaluation details are in Appendix A.5.2. For this comparison, we show frame and video accuracy, averaged over all the videos from all tasks across all test users (17 test users, 85 tasks in total). We also report the number of shared and individual updateable parameters required to be stored or transmitted. The key observations from our results are:

- FiT-LDA outperforms competitive meta-learning methods, Simple CNAPs and ProtoNets.
- FiT-LDA also outperforms FineTuner in terms of the video accuracy and performs within error bars of it in terms of the frame accuracy.
- The number of individual parameters for FiT-LDA is far fewer than in Simple CNAPs and is of the same order of magnitude as FineTuner and ProtoNets.
- Compared to a linear head, Naive Bayes reduces the size of the optimization space as there are fewer parameters to learn (only  $\psi$  and  $e$ ), making FiT-LDA more suitable for the few-shot setting.

#### 4.4 Few-shot Federated Learning

In this section, we show how FiT can be used in the few-shot federated learning setting, where training data are split between client nodes, e.g. mobile phones or personal laptops, and each client has only a handful of samples. Model training is performed via numerous communication rounds between a server and clients. In each round, the server selects a fraction of clients making updates and then sends the current model parameters to these clients. For data privacy reasons, clients update models locally using only their personal data and then send their parameter updates back to the server. Finally, the server aggregates information from all the clients, updates the shared model parameters, and proceeds to the next round until convergence. In this setting, models with a smaller number of updateable parameters are preferred in order to reduce the client-server communication cost which is typically bandwidth-limited.

**Experiments** For our experiments, we use CIFAR100 [32], a relatively large-scale dataset compared to those commonly used to benchmark federated learning methods [49, 50]. We employ the basic FedAvg [51] algorithm. We train all models for 60 communication rounds, with 5 clients per round and 10 update steps per client. Each client has 10 classes, which are sampled randomly before the start of training. During an update, a client initializes their local model with recent FiLM parameters received from the server and then performs several training steps as described in Section 2, using only their data. The Naive Bayes head allows a client to construct a local classifier at each update step, eliminating the need to initiate a shared classifier and transmit the parameters of this classifier at each training round. In contrast, using a linear head in this setting would entail additional communication costs, as it would be passed at each client-server interaction. We use a ProtoNets head for simplicity, although QDA and LDA heads could also be used. After training, the global FiLM parameters are transmitted to all clients. More specific training and evaluation details are in Appendix A.5.3.

We evaluate FiT in two scenarios, global and personalized. In the global setting, the aim is to construct a global classifier and report accuracy on the CIFAR100 [32] test set. We assume that the server knows which classes belong to each client, and constructs a shared classifier by taking a mean over prototypes produced by clients for a particular class. In the personalized scenario, we test a personalized model on test classes present in the individual’s training set and then report the mean accuracy over all clients. As opposed to the personalization experiments on ORBIT, where a personalized model is trained using only the client’s local data, in this experiment we initialize a personalized model with the learned global FiLM parameters and then construct a ProtoNets classifier with individual’s data. Thus, the goal of the personalized setting is to estimate how advantageous distributed learning can be for training FiLM layers to build personalized few-shot models.

To evaluate the FiT model in a distributed learning setup, we define baselines which form an upper and lower bounds on the model performance. For the global scenario, we take a FiT model simultaneously trained on all available data as the upper bound baseline. To get the lower bound baseline, we train a FiT model for each client with their local data, then average FiLM parameters of these individual models and construct a global ProtoNets classifier using the resulting FiLM parameters. The upper bound is therefore standard batch training, the performance of which we hope federated learning can approach. The lower bound is a simplistic version of federated learning with a single communication round which federated averaging should improve over. For the personalized setting, the upper bound baseline is as in the global scenario from which we form a personalized classifier by taking a subset of classes belonging to a client from a global 100-way classifier. The lower bound baseline is set to a FiT model trained for each client individually. The upper bound is again standard batch training and the lower bound is derived from locally trained models which do not share information and therefore should be improved upon by federated learning.

**Results** Fig. 2 shows global and personalized classification accuracy as a function of communication cost for different numbers of clients and shots per client. By communication cost we mean the number of parameters transmitted during training. The key observations from our results are:

- In the global setting, the federated learning model is only slightly worse (3 – 5%) than the upper bound baseline, while outperforming the lower bound model, often by a large margin. This shows that FiT can be efficiently used in distributed learning settings with different configurations.
- In the personalized scenario, for a sufficient number of clients ( $\geq 50$ ) the gap between the federated learning model and the upper bound model is significantly reduced with the increase in number of shots. Distributed training strongly outperforms the lower bound baseline, surprisingly even in the case of 10 clients with disjoint classes. This provides empirical evidence that collaborative distributed training can be helpful for improving personalized models in the few-shot data regime.
- The low communication cost per round and relatively fast empirical convergence of FiT results in a parameter efficient training protocol, requiring only around 7M parameters to be transferred during the whole training phase. In contrast, if we use BiT for federated learning, around 235M parameters will be sent at each communication round, yielding an enormous communication cost.

In Appendix A.3.4, we show that distributed training of a FiT model can be efficiently used to learn from more extreme, non-natural image datasets like Quickdraw [52]. Although the number of communication rounds must be increased for efficient transfer to Quickdraw, FiT still has orders of magnitude lower communication cost than BiT.

## 5 Discussion

In this work, we proposed FiT, a parameter and data efficient few-shot transfer learning system that allows image classification models to be updated with only a small subset of the total model parameters. We demonstrated that FiT can outperform BiT, a state-of-the-art transfer learning method at low shot while using one hundred times fewer updateable parameters. We also showed the efficiency benefits of employing FiT in model personalization and federated learning applications. There has been considerable work on compressing models [53] and designing more parameter efficient networks [54–56] to reduce the model parameter count. These lines of research are complementary to FiT. Model compression can be used in conjunction with our work by compressing the subset of updateable parameters. Similarly, parameter efficient networks can serve as the backbones of our classification systems. We leave the combination of these technologies and FiT for future work.



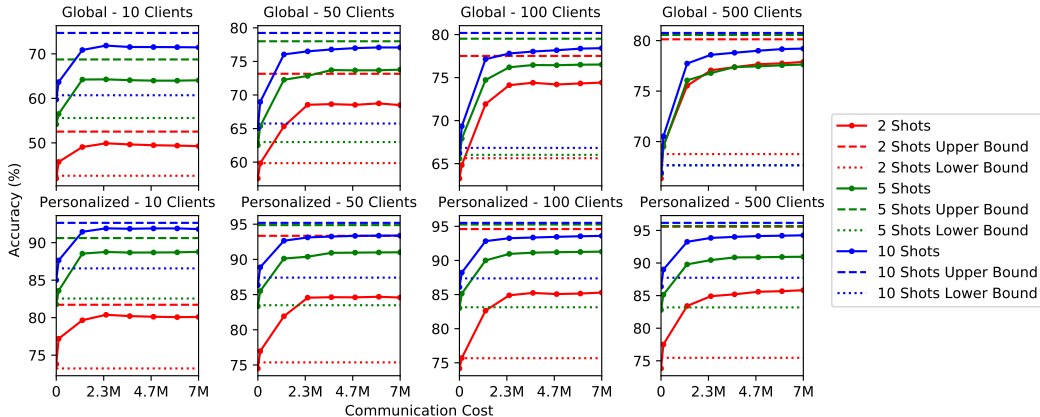


Figure 2: Global and personalized classification accuracy as a function of communication cost over 60 rounds for different numbers of clients and shots per client on CIFAR100. Classification accuracy is on the vertical axis and is the average of 3 runs with different data sampling seeds. The color of the line indicates the number of shots per class. The solid line shows the federated learning model, while dashed and dotted lines indicate the upper and lower bounds baselines, respectively.

**Limitations** The main limitation of this work is that it is computationally expensive and much slower to adapt to new tasks compared to meta-learning methods that can adapt with a single forward pass through a network [9] or a small number of gradient steps [57]. Thus FiT may be inappropriate for certain time critical applications and potentially use more energy than competitive approaches.

**Societal Impact** Image classification methods, including the work presented here, have the potential to be beneficial to society as they are readily applicable to medical image analysis, remote sensing for environmental work, and as we demonstrated in Section 4.3, helping blind users find their personal items. Conversely, the same methods could be deployed in an adverse manner such as in military or police surveillance systems. Our system for improving the parameter efficiency of models has the potential benefits of lowering energy, bandwidth, and storage costs and our federating learning approach may provide benefits in protecting user privacy. Despite the improvements presented in this work, image classification methods remain imperfect and can potentially capture biases that violate fairness principles. As a result, our method should be applied judiciously.

## 6 Acknowledgements

We thank Aristeidis Panos and Siddharth Swaroop for providing helpful and insightful comments. This work has been performed using resources provided by the Cambridge Tier-2 system operated by the University of Cambridge Research Computing Service <https://www.hpc.cam.ac.uk> funded by EPSRC Tier-2 capital grant EP/P020259/1.

## Funding Transparency Statement

Funding in direct support of this work: Aliaksandra Shysheya, John Bronskill, Massimiliano Patacchiola and Richard E. Turner are supported by an EPSRC Prosperity Partnership EP/T005386/1 between the EPSRC, Microsoft Research and the University of Cambridge.

## References

- [1] Florian Schroff, Dmitry Kalenichenko, and James Philbin. Facenet: A unified embedding for face recognition and clustering. In *Proceedings of the IEEE conference on computer vision and pattern recognition*, pages 815–823, 2015.
- [2] Tom Brown, Benjamin Mann, Nick Ryder, Melanie Subbiah, Jared D Kaplan, Prafulla Dhariwal, Arvind Neelakantan, Pranav Shyam, Girish Sastry, Amanda Askell, et al. Language models are few-shot learners. *Advances in neural information processing systems*, 33:1877–1901, 2020.

- [3] Wayne Xiong, Lingfeng Wu, Fil Allewa, Jasha Droppo, Xuedong Huang, and Andreas Stolcke. The microsoft 2017 conversational speech recognition system. In *2018 IEEE international conference on acoustics, speech and signal processing (ICASSP)*, pages 5934–5938. IEEE, 2018.
- [4] Yonghui Wu, Mike Schuster, Zhifeng Chen, Quoc V Le, Mohammad Norouzi, Wolfgang Macherey, Maxim Krikun, Yuan Cao, Qin Gao, Klaus Macherey, et al. Google’s neural machine translation system: Bridging the gap between human and machine translation. *arXiv preprint arXiv:1609.08144*, 2016.
- [5] Daniela Massiceti, Luisa Zintgraf, John Bronskill, Lida Theodorou, Matthew Tobias Harris, Edward Cutrell, Cecily Morrison, Katja Hofmann, and Simone Stumpf. ORBIT: A Real-World Few-Shot Dataset for Teachable Object Recognition. In *Proceedings of the IEEE/CVF International Conference on Computer Vision (ICCV)*, 2021.
- [6] Brendan McMahan, Eider Moore, Daniel Ramage, Seth Hampson, and Blaise Aguera y Arcas. Communication-efficient learning of deep networks from decentralized data. In *Artificial intelligence and statistics*, pages 1273–1282. PMLR, 2017.
- [7] Timothy Hospedales, Antreas Antoniou, Paul Micaelli, and Amos Storkey. Meta-learning in neural networks: A survey. *arXiv preprint arXiv:2004.05439*, 2020.
- [8] Jason Yosinski, Jeff Clune, Yoshua Bengio, and Hod Lipson. How transferable are features in deep neural networks? In *Proceedings of the 28th Annual Conference on Neural Information Processing Systems (NeurIPS)*, pages 3320–3328, 2014.
- [9] James Requeima, Jonathan Gordon, John Bronskill, Sebastian Nowozin, and Richard E Turner. Fast and flexible multi-task classification using conditional neural adaptive processes. In *Proceedings of the 33rd Annual Conference on Neural Information Processing Systems (NeurIPS)*, pages 7957–7968, 2019.
- [10] Vincent Dumoulin, Neil Houlsby, Utku Evci, Xiaohua Zhai, Ross Goroshin, Sylvain Gelly, and Hugo Larochelle. Comparing transfer and meta learning approaches on a unified few-shot classification benchmark. *arXiv preprint arXiv:2104.02638*, 2021.
- [11] Yonglong Tian, Yue Wang, Dilip Krishnan, Joshua B. Tenenbaum, and Phillip Isola. Rethinking few-shot image classification: a good embedding is all you need? *arXiv preprint arXiv:2003.11539*, 2020.
- [12] Alexander Kolesnikov, Lucas Beyer, Xiaohua Zhai, Joan Puigcerver, Jessica Yung, Sylvain Gelly, and Neil Houlsby. Big transfer (bit): General visual representation learning. *arXiv preprint arXiv:1912.11370*, 6(2):8, 2019.
- [13] Marton Havasi, Rodolphe Jenatton, Stanislav Fort, Jeremiah Zhe Liu, Jasper Snoek, Balaji Lakshminarayanan, Andrew M Dai, and Dustin Tran. Training independent subnetworks for robust prediction. *arXiv preprint arXiv:2010.06610*, 2020.
- [14] Ethan Perez, Florian Strub, Harm De Vries, Vincent Dumoulin, and Aaron Courville. FiLM: Visual reasoning with a general conditioning layer. In *Proceedings of the 32nd AAAI Conference on Artificial Intelligence (AAAI)*, 2018.
- [15] Kaiming He, Xiangyu Zhang, Shaoqing Ren, and Jian Sun. Deep residual learning for image recognition. In *Proceedings of the IEEE/CVF Conference on Computer Vision and Pattern Recognition (CVPR)*, pages 770–778, 2016.
- [16] Olga Russakovsky, Jia Deng, Hao Su, Jonathan Krause, Sanjeev Satheesh, Sean Ma, Zhiheng Huang, Andrej Karpathy, Aditya Khosla, Michael Bernstein, Alexander C. Berg, and Li Fei-Fei. ImageNet Large Scale Visual Recognition Challenge. *International Journal of Computer Vision (IJCV)*, 115(3):211–252, 2015. doi: 10.1007/s11263-015-0816-y.
- [17] Kaiming He, Xiangyu Zhang, Shaoqing Ren, and Jian Sun. Identity mappings in deep residual networks. In *European conference on computer vision*, pages 630–645. Springer, 2016.

- [18] Trevor Hastie, Robert Tibshirani, and Jerome Friedman. *The elements of statistical learning: data mining, inference, and prediction*. Springer Science & Business Media, 2009.
- [19] Bradley Efron. The efficiency of logistic regression compared to normal discriminant analysis. *Journal of the American Statistical Association*, 70(352):892–898, 1975.
- [20] Maja Pohar, Mateja Blas, and Sandra Turk. Comparison of logistic regression and linear discriminant analysis: a simulation study. *Metodoloski zvezki*, 1(1):143, 2004.
- [21] Ronald A Fisher. The use of multiple measurements in taxonomic problems. *Annals of eugenics*, 7(2):179–188, 1936.
- [22] Richard O Duda, Peter E Hart, and David G Stork. *Pattern classification*. John Wiley & Sons, 2012.
- [23] Jake Snell, Kevin Swersky, and Richard Zemel. Prototypical networks for few-shot learning. In *Proceedings of the 31st Annual Conference on Neural Information Processing Systems (NeurIPS)*, pages 4077–4087, 2017.
- [24] Oriol Vinyals, Charles Blundell, Timothy Lillicrap, Koray Kavukcuoglu, and Daan Wierstra. Matching networks for one shot learning. In *Proceedings of the 30th Annual Conference on Neural Information Processing Systems (NeurIPS)*, pages 3630–3638, 2016.
- [25] Sylvestre-Alvise Rebuffi, Hakan Bilen, and Andrea Vedaldi. Learning multiple visual domains with residual adapters. In *Advances in Neural Information Processing Systems*, pages 506–516, 2017.
- [26] Sylvestre-Alvise Rebuffi, Hakan Bilen, and Andrea Vedaldi. Efficient parametrization of multi-domain deep neural networks. In *Proceedings of the IEEE Conference on Computer Vision and Pattern Recognition*, pages 8119–8127, 2018.
- [27] Peyman Bateni, Raghav Goyal, Vaden Masrani, Frank Wood, and Leonid Sigal. Improved few-shot visual classification. In *Proceedings of the IEEE/CVF Conference on Computer Vision and Pattern Recognition (CVPR)*, pages 14493–14502, 2020.
- [28] John F Bronskill, Daniela Massiceti, Massimiliano Patacchiola, Katja Hofmann, Sebastian Nowozin, and Richard E Turner. Memory efficient meta-learning with large images. In *Thirty-Fifth Conference on Neural Information Processing Systems*, 2021. URL [https://openreview.net/forum?id=x2pF7Tt\\_S5u](https://openreview.net/forum?id=x2pF7Tt_S5u).
- [29] Eleni Triantafillou, Hugo Larochelle, Richard Zemel, and Vincent Dumoulin. Learning a universal template for few-shot dataset generalization. In *International Conference on Machine Learning*, pages 10424–10433. PMLR, 2021.
- [30] Pramod Kaushik Mudrakarta, Mark Sandler, Andrey Zhmoginov, and Andrew Howard. K for the price of 1: Parameter efficient multi-task and transfer learning. In *International Conference on Learning Representations*, 2019. URL <https://openreview.net/forum?id=BJxvEh0cFQ>.
- [31] Xiaohua Zhai, Joan Puigcerver, Alexander Kolesnikov, Pierre Ruysen, Carlos Riquelme, Mario Lucic, Josip Djolonga, Andre Susano Pinto, Maxim Neumann, Alexey Dosovitskiy, et al. A large-scale study of representation learning with the visual task adaptation benchmark. *arXiv preprint arXiv:1910.04867*, 2019.
- [32] Alex Krizhevsky, Geoffrey Hinton, et al. Learning multiple layers of features from tiny images. 2009.
- [33] Maria-Elena Nilsback and Andrew Zisserman. Automated flower classification over a large number of classes. In *2008 Sixth Indian Conference on Computer Vision, Graphics & Image Processing*, pages 722–729. IEEE, 2008.
- [34] Omkar M Parkhi, Andrea Vedaldi, Andrew Zisserman, and CV Jawahar. Cats and dogs. In *2012 IEEE conference on computer vision and pattern recognition*, pages 3498–3505. IEEE, 2012.
- [35] Li Fei-Fei, Rob Fergus, and Pietro Perona. One-shot learning of object categories. *IEEE transactions on pattern analysis and machine intelligence*, 28(4):594–611, 2006.

- [36] Jianxiong Xiao, James Hays, Krista A Ehinger, Aude Oliva, and Antonio Torralba. Sun database: Large-scale scene recognition from abbey to zoo. In *2010 IEEE computer society conference on computer vision and pattern recognition*, pages 3485–3492. IEEE, 2010.
- [37] Yuval Netzer, Tao Wang, Adam Coates, Alessandro Bissacco, Bo Wu, and Andrew Y Ng. Reading digits in natural images with unsupervised feature learning. 2011.
- [38] Mircea Cimpoi, Subhransu Maji, Iasonas Kokkinos, Sammy Mohamed, and Andrea Vedaldi. Describing textures in the wild. In *Proceedings of the IEEE conference on computer vision and pattern recognition*, pages 3606–3613, 2014.
- [39] Patrick Helber, Benjamin Bischke, Andreas Dengel, and Damian Borth. Eurosat: A novel dataset and deep learning benchmark for land use and land cover classification. *IEEE Journal of Selected Topics in Applied Earth Observations and Remote Sensing*, 12(7):2217–2226, 2019.
- [40] Gong Cheng, Junwei Han, and Xiaoqiang Lu. Remote sensing image scene classification: Benchmark and state of the art. *Proceedings of the IEEE*, 105(10):1865–1883, 2017.
- [41] Bastiaan S Veeling, Jasper Linmans, Jim Winkens, Taco Cohen, and Max Welling. Rotation equivariant cnns for digital pathology. In *International Conference on Medical image computing and computer-assisted intervention*, pages 210–218. Springer, 2018.
- [42] Kaggle and EyePacs. Kaggle diabetic retinopathy detection. <https://www.kaggle.com/c/diabetic-retinopathy-detection/data>, 2015.
- [43] Justin Johnson, Bharath Hariharan, Laurens Van Der Maaten, Li Fei-Fei, C Lawrence Zitnick, and Ross Girshick. Clevr: A diagnostic dataset for compositional language and elementary visual reasoning. In *Proceedings of the IEEE conference on computer vision and pattern recognition*, pages 2901–2910, 2017.
- [44] Loic Matthey, Irina Higgins, Demis Hassabis, and Alexander Lerchner. dsprites: Disentanglement testing sprites dataset, 2017.
- [45] Yann LeCun, Fu Jie Huang, and Leon Bottou. Learning methods for generic object recognition with invariance to pose and lighting. In *Proceedings of the 2004 IEEE Computer Society Conference on Computer Vision and Pattern Recognition, 2004. CVPR 2004.*, volume 2, pages II–104. IEEE, 2004.
- [46] Charles Beattie, Joel Z Leibo, Denis Teplyashin, Tom Ward, Marcus Wainwright, Heinrich Küttler, Andrew Lefrancq, Simon Green, Víctor Valdés, Amir Sadik, et al. Deepmind lab. *arXiv preprint arXiv:1612.03801*, 2016.
- [47] Andreas Geiger, Philip Lenz, Christoph Stiller, and Raquel Urtasun. Vision meets robotics: The kitti dataset. *The International Journal of Robotics Research*, 32(11):1231–1237, 2013.
- [48] Jia Deng, Wei Dong, Richard Socher, Li-Jia Li, Kai Li, and Li Fei-Fei. ImageNet: A large-scale hierarchical image database. In *Proceedings of the IEEE/CVF Conference on Computer Vision and Pattern Recognition (CVPR)*, 2009.
- [49] Sashank J. Reddi, Zachary Charles, Manzil Zaheer, Zachary Garrett, Keith Rush, Jakub Konečný, Sanjiv Kumar, and Hugh Brendan McMahan. Adaptive federated optimization. In *International Conference on Learning Representations*, 2021. URL <https://openreview.net/forum?id=LkFG31B13U5>.
- [50] Aviv Shamsian, Aviv Navon, Ethan Fetaya, and Gal Chechik. Personalized federated learning using hypernetworks. In *ICML*, 2021.
- [51] H. Brendan McMahan, Eider Moore, Daniel Ramage, and Blaise Agüera y Arcas. Federated learning of deep networks using model averaging. *CoRR*, abs/1602.05629, 2016. URL <http://arxiv.org/abs/1602.05629>.
- [52] J. Jongejan, H. Rowley, T. Kawashima, J. Kim, and N. Fox-Gieg. The quick, draw! - a.i. experiment. <https://quickdraw.withgoogle.com/data>, 2016.

- [53] Yu Cheng, Duo Wang, Pan Zhou, and Tao Zhang. A survey of model compression and acceleration for deep neural networks. arxiv 2017. *arXiv preprint arXiv:1710.09282*, 2017.
- [54] Mingxing Tan and Quoc Le. EfficientNet: Rethinking model scaling for convolutional neural networks. In *Proceedings of the 36th International Conference on Machine Learning (ICML)*, pages 6105–6114, 2019.
- [55] Mingxing Tan and Quoc Le. Efficientnetv2: Smaller models and faster training. In *International Conference on Machine Learning*, pages 10096–10106. PMLR, 2021.
- [56] Mark Sandler, Andrew Howard, Menglong Zhu, Andrey Zhmoginov, and Liang-Chieh Chen. Mobilenetv2: Inverted residuals and linear bottlenecks. In *Proceedings of the IEEE/CVF Conference on Computer Vision and Pattern Recognition (CVPR)*, pages 4510–4520, 2018.
- [57] Chelsea Finn, Pieter Abbeel, and Sergey Levine. Model-agnostic meta-learning for fast adaptation of deep networks. In *Proceedings of the 34th International Conference on Machine Learning (ICML)*, pages 1126–1135, 2017.
- [58] Diederik Kingma and Jimmy Ba. Adam: A method for stochastic optimization. In *Proceedings of the 3rd International Conference on Learning Representations (ICLR)*, 2015.
- [59] Alexander Kolesnikov, Lucas Beyer, Xiaohua Zhai, Joan Puigcerver, Jessica Yung, Sylvain Gelly, and Neil Houlsby. Official repository for the "Big Transfer (BiT): General Visual Representation Learning" paper. [https://github.com/google-research/big\\_transfer](https://github.com/google-research/big_transfer), 2020.

## A Appendix

### A.1 FiLM Layer Placement

Fig. A.1a illustrates a FiLM layer operating on a convolutional layer, and Fig. A.1b illustrates how a FiLM layer can be added to a ResNetV2 network block. FiLM layers can be similarly added to EfficientNet based backbones, amongst others.

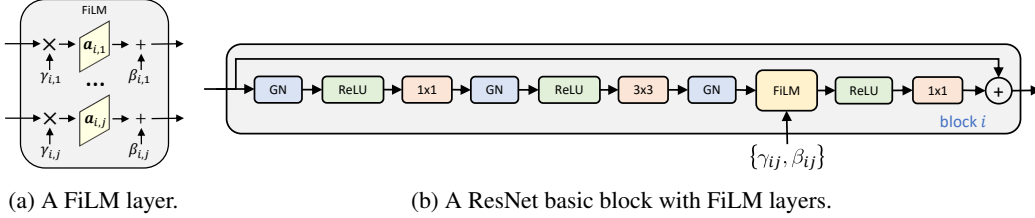


Figure A.1: (Left) A FiLM layer operating on convolutional feature maps in layer  $i$  and channel  $j$ . (Right) How a FiLM layer is placed within a basic Residual network block [15]. GN is a Group Normalization layer, ReLU is a Rectified Linear Unit, and  $1 \times 1$ , and  $3 \times 3$  are 2D convolutional layers with the stated kernel size.

### A.2 Model Parameters

Table A.1 depicts the shared and updateable parameters for BiT and the 3 variants of FiT as a function of  $\theta$ ,  $\psi$ ,  $d_b$ , and  $C$ . The rightmost column provides the example updateable parameter count for all models in the case of a BiT-M-R50x1 backbone with  $|\theta| = 23, 500, 352$ ,  $\psi = 11, 648$ ,  $d_b = 2048$ , and  $C = 10$ .

For FiT-QDA and FiT-LDA, the means and covariances contribute to the updateable parameter count. We use a mean for every class which contributes  $Cd_b$  updateable parameters. A covariance matrix has  $d_b \times d_b$  values, however it can be represented in Cholesky factorized form which results in a lower triangular matrix and thus can be represented with  $n(n+1)/2$  values, with the rest being zeros.

In the case of FiT-LDA, where the covariance matrix is shared across all classes, a more compact representation is possible, resulting in considerable savings in updateable parameters:

$$\begin{aligned}
 p(y^* = c | b_{\theta, \psi}(\mathbf{x}^*), \boldsymbol{\pi}, \boldsymbol{\mu}, \Sigma_{LDA}) &= \frac{\pi_c \mathcal{N}(b_{\theta, \psi}(\mathbf{x}^*) | \mu_c, \Sigma_{LDA})}{\sum_{c'} \pi_{c'} \mathcal{N}(b_{\theta, \psi}(\mathbf{x}^*) | \mu_{c'}, \Sigma_{LDA})} \\
 &= \frac{\pi_c \det(2\pi \Sigma_{LDA})^{-\frac{1}{2}} \exp\left(-\frac{1}{2} (b_{\theta, \psi}(\mathbf{x}^*) - \mu_c)^T \Sigma_{LDA}^{-1} (b_{\theta, \psi}(\mathbf{x}^*) - \mu_c)\right)}{\sum_{c'} \pi_{c'} \det(2\pi \Sigma_{LDA})^{-\frac{1}{2}} \exp\left(-\frac{1}{2} (b_{\theta, \psi}(\mathbf{x}^*) - \mu_{c'})^T \Sigma_{LDA}^{-1} (b_{\theta, \psi}(\mathbf{x}^*) - \mu_{c'})\right)} \quad (\text{A.1}) \\
 &= \frac{\pi_c \exp\left(-\frac{1}{2} b_{\theta, \psi}(\mathbf{x}^*)^T \Sigma_{LDA}^{-1} b_{\theta, \psi}(\mathbf{x}^*) + \mu_c^T \Sigma_{LDA}^{-1} b_{\theta, \psi}(\mathbf{x}^*) - \frac{1}{2} \mu_c^T \Sigma_{LDA}^{-1} \mu_c\right)}{\sum_{c'} \pi_{c'} \exp\left(-\frac{1}{2} b_{\theta, \psi}(\mathbf{x}^*)^T \Sigma_{LDA}^{-1} b_{\theta, \psi}(\mathbf{x}^*) + \mu_{c'}^T \Sigma_{LDA}^{-1} b_{\theta, \psi}(\mathbf{x}^*) - \frac{1}{2} \mu_{c'}^T \Sigma_{LDA}^{-1} \mu_{c'}\right)} \\
 &= \frac{\pi_c \exp\left(\mu_c^T \Sigma_{LDA}^{-1} b_{\theta, \psi}(\mathbf{x}^*) - \frac{1}{2} \mu_c^T \Sigma_{LDA}^{-1} \mu_c\right)}{\sum_{c'} \pi_{c'} \exp\left(\mu_{c'}^T \Sigma_{LDA}^{-1} b_{\theta, \psi}(\mathbf{x}^*) - \frac{1}{2} \mu_{c'}^T \Sigma_{LDA}^{-1} \mu_{c'}\right)}
 \end{aligned}$$

From Eq. (A.1), it follows that to compute the probability of classifying a test point  $\mathbf{x}^*$ , we need to store  $\mu_c^T \Sigma_{LDA}^{-1}$  which has dimensionality  $d_b$  and  $\mu_c^T \Sigma_{LDA}^{-1} \mu_c$  which has dimensionality 1 for each class  $c$ , resulting in only  $C(d_b + 1)$  parameters required for the FiT-LDA head. Since the covariance matrix is not shared in the case of FiT-QDA, no additional savings are possible in that case.

### A.3 Additional Results

This section contains additional results that would not fit into the main paper, including tabular versions of figures.

Table A.1: Shared and updateable parameters for the transfer learning methods considered. The Example column contains the updateable parameters for all methods using a BiT-M-R50x1 backbone with  $|\theta| = 23, 500, 352$ ,  $\psi = 11, 648$ ,  $d_b = 2048$ , and  $C = 10$ .

Method	Shared	Updateable	Example
BiT	0	$ \theta  +  \phi  =  \theta  + Cd_b$	23,520,832
FiT - QDA	$ \theta $	$ \psi  +  \mu  +  \Sigma  +  e  =  \psi  + Cd_b + C \frac{d_b(d_b+1)}{2} + 3$	21,013,891
FiT - LDA	$ \theta $	$ \psi  + ( \mu  +  \Sigma ) +  e  =  \psi  + C(d_b + 1) + 2$	32,140
FiT - ProtoNets	$ \theta $	$ \psi  +  \mu  =  \psi  + Cd_b$	32,128

### A.3.1 Additional Few-shot Results

Table A.2 shows the tabular version of Fig. 1. In addition, Table A.2 includes results for an additional variant of BiT (BiT-FiLM), and two additional variants of FiT (FiT-QDA and FiT-ProtoNets). Refer to Section 4.1 for analysis.

Table A.2: Classification accuracy and Relative Model Update Size (RMUS) for all three variants of FiT and two variants of BiT on standard downstream datasets as a function of shots per class. The backbone is BiT-M-R50x1 with  $|\theta| = 23, 500, 352$ ,  $\psi = 11, 648$ , and  $d_b = 2048$ . Accuracy figures are percentages and the  $\pm$  sign indicates the 95% confidence interval over 3 runs. Bold type indicates the highest scores (within the confidence interval).

Dataset	C	Shot	BiT				FiLM Transfer (FiT)					
			Standard		FiLM		QDA		LDA		ProtoNets	
			Accuracy	RMUS	Accuracy	RMUS	Accuracy	RMUS	Accuracy	RMUS	Accuracy	RMUS
CIFAR10 [32]	10	1	<b>52.7±3.9</b>	1.0	<b>47.0±14.2</b>	0.0014	<b>54.0±5.7</b>	0.893	<b>54.0±5.7</b>	0.0014	<b>52.9±5.0</b>	0.0014
	10	2	<b>69.9±2.6</b>	1.0	<b>63.4±3.6</b>	0.0014	<b>73.0±8.8</b>	0.893	<b>74.2±8.8</b>	0.0014	<b>68.9±9.4</b>	0.0014
	10	5	<b>83.5±3.0</b>	1.0	<b>82.8±1.9</b>	0.0014	<b>85.4±3.9</b>	0.893	<b>86.4±4.2</b>	0.0014	<b>81.8±5.1</b>	0.0014
	10	10	<b>88.1±2.0</b>	1.0	46.1±39.7	0.0014	<b>89.5±1.3</b>	0.893	<b>90.6±1.0</b>	0.0014	87.3±2.3	0.0014
	10	All	95.9±0.2	1.0	96.0±0.2	0.0014	<b>96.4±0.0</b>	0.893	96.3±0.1	0.0014	96.0±0.1	0.0014
CIFAR100 [32]	100	1	<b>36.4±1.3</b>	1.0	30.2±2.7	0.0091	33.8±0.8	8.860	33.8±0.8	0.0091	30.7±0.7	0.0091
	100	2	48.8±0.2	1.0	43.0±2.9	0.0091	<b>55.1±1.1</b>	8.860	<b>54.5±1.0</b>	0.0091	50.6±1.8	0.0091
	100	5	65.3±1.5	1.0	39.6±0.6	0.0091	<b>69.0±0.7</b>	8.860	<b>69.5±1.3</b>	0.0091	<b>67.9±0.7</b>	0.0091
	100	10	72.3±0.9	1.0	50.1±0.2	0.0091	<b>75.6±0.6</b>	8.860	<b>75.3±0.6</b>	0.0091	74.7±0.3	0.0091
	100	All	<b>86.1±0.1</b>	1.0	82.6±0.2	0.0091	82.1±0.1	8.860	82.6±0.2	0.0091	80.3±0.4	0.0091
Flowers102 [33]	102	1	79.8±0.7	1.0	79.3±2.5	0.0093	<b>89.6±0.9</b>	9.036	<b>89.6±0.9</b>	0.0093	85.1±0.9	0.0093
	102	2	89.6±1.4	1.0	91.7±0.8	0.0093	<b>95.6±0.5</b>	9.036	<b>95.6±0.7</b>	0.0093	93.0±0.9	0.0093
	102	5	96.8±0.7	1.0	96.3±0.2	0.0093	<b>98.3±0.3</b>	9.036	<b>98.4±0.3</b>	0.0093	<b>98.0±0.3</b>	0.0093
	102	10	97.3±0.7	1.0	96.9±0.7	0.0093	<b>99.0±0.1</b>	9.036	98.8±0.1	0.0093	98.6±0.1	0.0093
	102	All	96.6±0.4	1.0	96.9±0.4	0.0093	<b>99.0±0.1</b>	9.036	<b>98.9±0.1</b>	0.0093	98.6±0.2	0.0093
Pets [34]	37	1	38.3±2.3	1.0	36.8±5.5	0.0037	<b>50.2±2.8</b>	3.297	<b>50.1±3.1</b>	0.0037	<b>46.6±2.0</b>	0.0037
	37	2	61.2±2.6	1.0	60.1±3.0	0.0037	<b>74.8±1.4</b>	3.297	<b>76.8±1.8</b>	0.0037	<b>72.8±2.7</b>	0.0037
	37	5	76.7±2.0	1.0	76.8±1.5	0.0037	80.0±0.2	3.297	<b>82.5±0.4</b>	0.0037	78.4±0.7	0.0037
	37	10	78.6±5.3	1.0	79.2±4.4	0.0037	<b>86.2±1.0</b>	3.297	<b>86.9±1.5</b>	0.0037	<b>85.8±0.4</b>	0.0037
	37	All	90.1±0.6	1.0	90.1±0.2	0.0037	<b>91.7±0.3</b>	3.297	<b>91.9±0.3</b>	0.0037	91.2±0.1	0.0037

### A.3.2 Few-shot Task Ablations

Table A.3 shows the few-shot results for all three variants of FiT with different ablations on how the downstream dataset  $\mathcal{D}$  is allocated during training. *No Split* indicates that  $\mathcal{D}_{train}$  is not split into two disjoint partitions and  $\mathcal{D}_{train} = \mathcal{D}_{test} = \mathcal{D}$ . However,  $\mathcal{D}_{train}$  and  $\mathcal{D}_{test}$  are sampled to form episodic training tasks as detailed in Algorithm A.2. *Split* indicates that  $\mathcal{D}_{train}$  is split into two disjoint partitions as detailed in Algorithm A.1 and then sampled into tasks as described in Algorithm A.2. *Use All* indicates that  $\mathcal{D}_{train} = \mathcal{D}_{test} = \mathcal{D}$  (i.e.  $\mathcal{D}$  is not split) and that  $\mathcal{D}_{train}$  and  $\mathcal{D}_{test}$  are not sampled and that  $\mathcal{D}_S^\tau = \mathcal{D}_Q^\tau = \mathcal{D}$  for all tasks  $\tau$ .

Table A.3 shows that *Use All* is consistently the worst option. In general, in the few-shot case, *Split* either outperforms *No Split* (CIFAR10, Pets) or achieves the same level of performance (CIFAR100, Flowers102). As a result, we use the *Split* option when reporting the few-shot results.

### A.3.3 VTAB-1k Task Ablations

Table A.4 shows the VTAB-1k results for all three variants of FiT with different ablations on how the downstream dataset  $\mathcal{D}$  is allocated during training. Refer to Appendix A.3.2 for the meanings

Table A.3: Classification accuracy for all three variants of FiT as a function of shots per class and how the downstream dataset  $\mathcal{D}$  is utilized during training on standard datasets. The backbone is BiT-M-R50x1 with  $|\theta| = 23, 500, 352$ ,  $\psi = 11, 648$ , and  $d_b = 2048$ . Accuracy figures are percentages and the  $\pm$  sign indicates the 95% confidence interval over 3 runs.

Dataset	Shot	QDA			LDA			ProtoNets		
		No Split	Split	Use All	No Split	Split	Use All	No Split	Split	Use All
CIFAR10 [32]	1	42.5±2.2	54.0±5.7	37.2±3.9	36.7±4.3	54.0±5.7	28.5±2.3	53.0±5.1	52.9±5.0	53.0±5.1
	2	62.8±4.8	73.0±8.8	68.2±5.4	60.4±1.6	74.2±8.8	40.8±5.2	65.2±4.5	68.9±9.4	65.2±4.5
	5	79.7±0.9	85.4±3.9	79.6±1.0	86.6±3.5	86.4±4.2	69.4±3.5	76.1±4.2	81.8±5.1	75.6±9.3
	10	84.2±0.1	89.5±1.3	84.0±0.3	92.3±0.3	90.6±1.0	87.3±0.9	84.5±3.8	87.3±2.3	81.9±4.5
	All	96.6±0.1	96.4±0.0	96.2±0.0	96.6±0.0	96.3±0.1	96.6±0.0	96.1±0.1	96.0±0.1	95.4±0.0
CIFAR100 [32]	1	33.0±3.9	33.8±0.8	33.0±0.8	32.8±2.7	33.8±0.8	33.8±0.8	30.7±0.7	30.7±0.7	30.7±0.7
	2	54.5±2.0	55.1±1.1	45.6±2.0	55.6±1.2	54.5±1.0	45.1±3.1	52.3±2.0	50.6±1.8	40.2±6.1
	5	69.7±1.0	69.0±0.7	57.9±0.4	69.8±1.0	69.5±1.3	57.6±1.8	68.7±1.5	67.9±0.7	56.6±4.2
	10	75.5±0.3	75.6±0.6	67.6±7.9	75.6±0.2	75.3±0.6	67.0±3.2	74.8±0.2	74.7±0.3	65.4±2.8
	All	82.4±0.1	82.1±0.1	77.2±0.1	82.6±0.2	82.6±0.2	81.1±0.1	80.6±0.2	80.3±0.4	78.2±0.1
Flowers102 [33]	1	86.1±0.5	89.6±0.9	89.1±0.8	82.1±0.8	89.6±0.9	89.6±0.9	85.1±0.9	85.1±0.9	85.1±0.9
	2	95.2±0.6	95.6±0.5	94.4±0.6	95.6±0.5	95.6±0.7	94.9±0.5	93.9±1.0	93.0±0.9	91.9±1.2
	5	98.4±0.2	98.3±0.3	98.2±0.4	98.5±0.2	98.4±0.3	97.4±0.4	98.1±0.4	98.0±0.3	96.6±0.6
	10	99.0±0.0	99.0±0.1	98.9±0.1	98.9±0.1	98.8±0.1	98.5±0.0	98.6±0.0	98.6±0.1	96.7±0.0
	All	99.1±0.1	99.0±0.1	98.8±0.0	99.0±0.1	98.9±0.1	98.4±0.0	98.8±0.1	98.6±0.2	96.7±0.0
Pets [34]	1	29.4±3.1	50.2±2.8	50.2±2.8	17.2±6.3	50.1±3.1	50.0±3.2	46.6±2.0	46.6±2.0	46.6±2.0
	2	53.0±2.1	74.8±1.4	64.2±0.7	49.4±5.7	76.8±1.8	53.4±2.0	60.1±0.4	72.8±2.7	60.1±0.4
	5	81.2±2.3	80.0±0.2	73.6±1.1	82.1±2.2	82.5±0.4	71.0±3.1	83.0±2.4	78.4±0.7	67.4±6.2
	10	87.3±1.0	86.2±1.0	80.0±6.2	87.1±0.8	86.9±1.5	81.6±1.6	87.1±1.2	85.8±0.4	79.2±2.0
	All	92.1±0.2	91.7±0.3	77.8±0.0	91.8±0.2	91.9±0.3	88.3±0.1	91.8±0.2	91.2±0.1	82.4±0.4

of *No Split*, *Split*, and *Use All*. With some minor exceptions, the *Use All* case performs the worst. The performance of the *No Split* and *Split* options is very close, with *No Split* being slightly better when averaged over all of the datasets. As a result, we use the *No Split* option when reporting the VTAB-1k results.

Table A.4: Classification accuracy for all three variants of FiT on the VTAB-1k benchmark as a function of how the downstream dataset  $\mathcal{D}$  is utilized during training. The backbone is BiT-M-R50x1. Accuracy figures are percentages and the  $\pm$  sign indicates the 95% confidence interval over 3 runs. Bold type indicates the highest scores.

Dataset	QDA			LDA			ProtoNets		
	No Split	Split	Use All	No Split	Split	Use All	No Split	Split	Use All
Caltech101 [35]	90.3±0.8	90.0±0.7	85.5±0.0	90.4±0.8	90.7±0.7	87.3±0.0	89.6±0.2	89.7±0.3	82.3±0.0
CIFAR100 [32]	74.1±0.1	74.8±0.3	63.4±0.0	74.2±0.5	74.1±0.4	69.0±0.0	73.9±0.3	73.7±0.6	65.5±0.2
Flowers102 [33]	99.1±0.1	99.0±0.1	98.8±0.0	99.0±0.1	98.9±0.1	98.5±0.0	98.6±0.0	98.6±0.1	96.7±0.0
Pets [34]	91.0±0.3	90.4±0.4	75.6±0.0	90.5±0.0	90.5±0.5	87.2±0.1	90.8±0.2	90.4±0.2	85.6±0.0
Sun397 [36]	51.1±0.7	52.1±0.1	49.3±0.7	51.6±0.5	50.8±0.7	42.7±3.4	51.5±1.4	50.4±0.8	42.4±4.2
SVHN [37]	75.1±1.3	73.3±1.4	26.2±0.1	74.2±0.9	71.5±0.2	67.4±0.0	50.1±2.2	47.4±1.4	35.1±0.1
DTD [38]	70.9±0.1	70.2±0.3	72.8±0.0	70.9±0.1	70.8±0.3	66.5±0.0	68.2±1.1	68.4±1.0	61.3±0.2
EuroSAT [39]	95.6±0.1	94.7±0.6	93.5±0.0	95.1±0.1	94.3±0.6	94.3±0.0	93.8±0.1	92.7±0.2	89.4±0.1
Resiscs45 [40]	82.6±0.1	82.0±0.3	77.5±0.0	82.5±0.2	80.8±0.2	78.3±0.1	77.0±0.0	76.4±0.8	71.9±0.1
Patch Camelyon [41]	80.7±1.2	81.5±1.0	65.7±0.0	82.5±0.7	80.5±0.8	82.4±0.5	79.9±0.2	78.5±2.1	69.0±0.1
Retinopathy [42]	70.4±0.1	67.5±1.0	25.5±0.0	66.2±0.5	63.4±0.3	25.0±0.1	57.9±0.3	58.4±0.6	17.0±0.0
CLEVR-count [43]	87.1±0.3	84.9±1.1	40.6±0.1	85.6±0.9	84.3±0.5	82.0±0.1	88.7±0.3	85.4±0.7	87.4±0.1
CLEVR-dist [43]	58.1±0.8	58.4±0.6	39.1±0.1	56.1±0.8	55.7±1.7	57.7±0.4	58.3±0.6	55.0±1.2	33.7±0.2
dSprites-loc [44]	77.1±2.0	75.1±1.2	13.5±0.3	74.8±1.4	71.1±1.1	62.4±1.1	68.6±2.4	66.8±0.8	74.8±1.4
dSprites-ori [44]	56.7±0.3	55.6±0.7	39.6±1.8	51.3±0.7	48.0±0.1	53.8±0.0	34.2±0.8	32.4±1.2	36.7±0.3
SmallNORB-azi [45]	18.9±0.6	19.8±0.6	14.0±0.1	16.2±0.1	17.1±1.3	15.8±0.3	13.5±0.1	13.0±0.6	13.1±0.0
SmallNORB-elev [45]	40.4±0.2	40.3±1.4	28.2±0.1	37.0±0.6	38.5±1.6	36.1±0.3	35.0±0.6	34.0±0.9	26.5±0.1
DMLab [46]	43.8±0.3	41.2±1.3	33.7±0.1	41.6±0.6	39.5±1.3	38.9±0.4	39.3±0.3	38.6±0.2	28.2±0.1
KITTI-dist [47]	77.5±0.7	77.2±2.2	73.6±0.1	77.7±0.8	77.5±1.3	73.1±0.1	75.3±0.2	74.3±2.9	69.0±0.9
All	<b>70.6</b>	69.9	53.5	<b>69.3</b>	68.3	64.1	<b>65.5</b>	64.4	57.1
Natural	<b>78.8</b>	78.5	67.4	<b>78.7</b>	78.2	74.1	<b>74.7</b>	74.1	67.0
Specialized	<b>82.3</b>	81.4	65.6	<b>81.5</b>	79.7	70.0	<b>77.1</b>	76.5	61.8
Structured	<b>57.5</b>	56.6	35.3	<b>55.0</b>	54.0	52.5	<b>51.6</b>	49.9	46.2



Table A.5: Few-shot Federated Learning Results on CIFAR100 for different numbers of clients and shots per client. Accuracy figures are percentages and the  $\pm$  sign indicates the 95% confidence interval over 3 runs. Global stands for the global setting, while Personalized stands for the personalized scenario. FL indicates Federated Learning training.

Clients	Shot	Global			Personalized		
		Lower Bound	FL	Upper Bound	Lower Bound	FL	Upper Bound
10	2	42.6 $\pm$ 1.9	49.3 $\pm$ 1.3	52.5 $\pm$ 0.9	73.2 $\pm$ 1.4	80.1 $\pm$ 0.8	81.7 $\pm$ 1.2
	5	55.6 $\pm$ 1.6	64.1 $\pm$ 1.6	68.7 $\pm$ 0.7	82.6 $\pm$ 0.4	88.8 $\pm$ 0.2	90.6 $\pm$ 0.4
	10	60.7 $\pm$ 1.2	71.5 $\pm$ 0.8	74.7 $\pm$ 0.3	86.6 $\pm$ 0.2	91.8 $\pm$ 0.5	92.6 $\pm$ 0.6
50	2	59.9 $\pm$ 0.6	68.5 $\pm$ 0.3	73.2 $\pm$ 0.2	75.4 $\pm$ 0.9	84.6 $\pm$ 0.5	93.4 $\pm$ 0.2
	5	63.0 $\pm$ 0.8	73.8 $\pm$ 0.7	78.0 $\pm$ 0.1	83.5 $\pm$ 0.5	91.0 $\pm$ 0.4	94.9 $\pm$ 0.2
	10	65.8 $\pm$ 1.1	77.1 $\pm$ 0.3	79.2 $\pm$ 0.3	87.4 $\pm$ 0.6	93.4 $\pm$ 0.3	95.2 $\pm$ 0.1
100	2	65.6 $\pm$ 0.6	74.4 $\pm$ 0.3	77.5 $\pm$ 0.2	75.7 $\pm$ 0.9	85.3 $\pm$ 0.2	94.6 $\pm$ 0.2
	5	66.0 $\pm$ 0.3	76.5 $\pm$ 0.2	79.5 $\pm$ 0.2	83.1 $\pm$ 0.9	91.3 $\pm$ 0.2	95.3 $\pm$ 0.1
	10	66.8 $\pm$ 0.3	78.4 $\pm$ 0.1	80.2 $\pm$ 0.1	87.4 $\pm$ 0.5	93.6 $\pm$ 0.2	95.5 $\pm$ 0.1
500	2	68.8 $\pm$ 0.1	77.9 $\pm$ 0.4	80.1 $\pm$ 0.3	75.5 $\pm$ 0.2	85.8 $\pm$ 0.2	95.6 $\pm$ 0.1
	5	67.6 $\pm$ 0.1	77.6 $\pm$ 0.1	80.6 $\pm$ 0.2	83.2 $\pm$ 0.3	91.0 $\pm$ 0.2	95.7 $\pm$ 0.1
	10	67.7 $\pm$ 0.1	79.2 $\pm$ 0.3	80.8 $\pm$ 0.2	87.7 $\pm$ 0.1	94.3 $\pm$ 0.1	96.2 $\pm$ 0.1

### A.3.4 Additional Few-shot Federated Learning Results

Table A.5 shows the tabular version of Fig. 2. For the Federated Learning results, it includes only the resulting accuracy after training for 60 communication rounds. Refer to Section 4.4 for analysis.

To test distributed training of a FiT model on a more extreme, non-natural image dataset, we also include the results for federated training of FiT on the Quickdraw dataset. As there is no pre-defined train/test split for the Quickdraw dataset, we randomly choose 100 samples from each of the 345 classes and use them for testing. We train all federated training models for 120 communication rounds, with 5 clients per round, and 10 update steps per client. Since Quickdraw is a more difficult dataset than CIFAR100, it requires more communication rounds for training. Each client has 35 classes, which are sampled randomly at the start of training. In our experiments, we omit the 10-clients case, as the overall amount of data in the system is not enough to even train a robust global upper bound baseline model.

Fig. A.2 shows global and personalized classification accuracy as a function of communication cost for different numbers of clients and shots per client for Quickdraw, while Table A.6 shows the tabular version of this figure.

Table A.6: Few-shot Federated Learning Results on Quickdraw for different numbers of clients and shots per client. Accuracy figures are percentages and the  $\pm$  sign indicates the 95% confidence interval over 3 runs. Global stands for the global setting, while Personalized stands for the personalized scenario. FL indicates Federated Learning training.

Clients	Shot	Global			Personalized		
		Lower Bound	FL	Upper Bound	Lower Bound	FL	Upper Bound
50	2	26.3 $\pm$ 0.4	29.0 $\pm$ 0.5	32.9 $\pm$ 0.6	36.9 $\pm$ 0.2	43.4 $\pm$ 0.6	64.2 $\pm$ 0.8
	5	30.6 $\pm$ 0.3	40.7 $\pm$ 0.6	43.9 $\pm$ 0.5	48.8 $\pm$ 0.4	63.6 $\pm$ 0.3	74.3 $\pm$ 0.4
	10	34.3 $\pm$ 0.7	44.9 $\pm$ 0.1	47.2 $\pm$ 0.2	56.5 $\pm$ 0.8	71.1 $\pm$ 0.1	76.6 $\pm$ 0.2
100	2	28.5 $\pm$ 0.1	32.4 $\pm$ 0.8	43.0 $\pm$ 1.0	35.9 $\pm$ 0.3	43.9 $\pm$ 1.0	73.1 $\pm$ 0.4
	5	32.8 $\pm$ 0.4	44.1 $\pm$ 0.4	47.4 $\pm$ 0.1	48.6 $\pm$ 0.9	64.9 $\pm$ 0.8	76.4 $\pm$ 0.3
	10	35.3 $\pm$ 0.1	46.8 $\pm$ 0.1	48.7 $\pm$ 0.2	55.5 $\pm$ 0.4	71.5 $\pm$ 0.5	77.2 $\pm$ 0.3
500	2	32.0 $\pm$ 0.3	40.3 $\pm$ 2.4	49.1 $\pm$ 0.3	36.2 $\pm$ 0.1	49.2 $\pm$ 2.4	77.6 $\pm$ 0.3
	5	34.0 $\pm$ 0.1	46.1 $\pm$ 0.1	48.6 $\pm$ 2.2	48.7 $\pm$ 0.2	65.8 $\pm$ 0.3	77.0 $\pm$ 1.7
	10	36.1 $\pm$ 0.1	48.1 $\pm$ 0.4	48.2 $\pm$ 1.2	55.7 $\pm$ 0.1	72.2 $\pm$ 0.2	76.7 $\pm$ 0.9

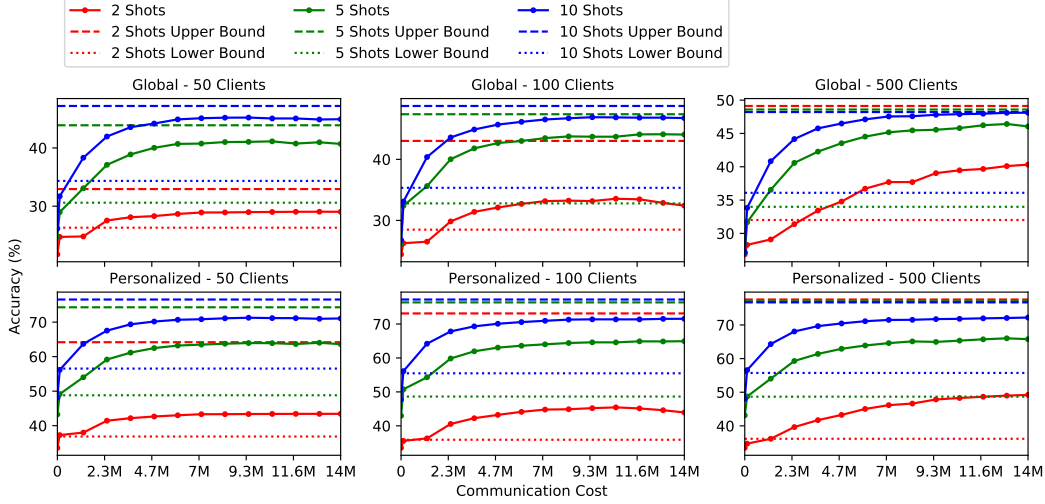


Figure A.2: Global and personalized classification accuracy as a function of communication cost over 120 rounds for different numbers of clients and shots per client on Quickdraw. Classification accuracy is on the vertical axis and is the average of 3 runs with different data sampling seeds. The color of the line indicates the number of shots per class. The solid line shows the federated learning model, while dashed and dotted lines indicate the upper and lower bounds baselines, respectively.

#### A.4 FIT Training Algorithms

Algorithm A.1 and Algorithm A.2 detail how episodic tasks are split and sampled, respectively, for use in the FIT training protocol.

---

##### Algorithm A.1 Splitting the downstream dataset $\mathcal{D}$

---

**Require:**  $\mathcal{D} = \{(x_n, y_n)\}_{n=1}^N = \{\mathbf{x}, \mathbf{y}\}$ : downstream dataset  
**Require:** `unique()`  $\equiv$  function that returns a list of unique classes and list of counts of each class  
**Require:** `select_by_class()`  $\equiv$  function that extracts samples of a specified class from a dataset

```

1: procedure SPLIT( $\mathcal{D}$ )
2:    $\mathcal{D}_{train} \leftarrow []$  ▷ Create an empty list to hold  $\mathcal{D}_{train}$ 
3:    $\mathcal{D}_{test} \leftarrow []$  ▷ Create an empty list to hold  $\mathcal{D}_{test}$ 
4:    $classes, class\_counts \leftarrow unique(\mathbf{y})$ 
5:   for all  $c \in classes$  do
6:      $assert(class\_counts(c) > 1)$  ▷ Require a minimum of 2 shots per class.
7:      $train\_count \leftarrow ceil(class\_counts(c)/2)$ 
8:      $\mathcal{D}_c \leftarrow select\_by\_class(c)$  ▷ Select examples of class  $c$  from  $\mathcal{D}$ 
9:      $\mathcal{D}_{train} \leftarrow \mathcal{D}_{train} + \mathcal{D}_c[:train\_count]$  ▷ Add  $train\_count$  examples to  $\mathcal{D}_{train}$ 
10:     $\mathcal{D}_{test} \leftarrow \mathcal{D}_{test} + \mathcal{D}_c[train\_count : ]$  ▷ Add remaining examples to  $\mathcal{D}_{test}$ 
11:   end for
12:   return  $\mathcal{D}_{train}, \mathcal{D}_{test}$ 
13: end procedure

```

---

#### A.5 Training and Evaluation Details

In this section, we provide implementation details for all of the experiments in Section 4.

##### A.5.1 Few-shot and VTAB-1k Transfer Learning Experiments

**FIT** All of the FIT few-shot and VTAB-1k transfer learning experiments were carried out on a single NVIDIA A100 GPU with 80GB of memory. The Adam optimizer [58] with a constant learning rate of 0.0035, for 400 iterations, and  $|\mathcal{D}_S^c|=100$  was used throughout. No data augmentation was used and images were scaled to  $384 \times 384$  pixels unless the image size was  $32 \times 32$  pixels or less, in

---

**Algorithm A.2** Sampling a task  $\tau$ 

---

**Require:**  $\mathcal{D}_{train} = \{(\mathbf{x}_s, \mathbf{y}_s)\}_{s=1}^{S_\tau} = \{\mathbf{x}_S, \mathbf{y}_S\}$ : train portion of downstream dataset  
**Require:**  $\mathcal{D}_{test} = \{(\mathbf{x}_q, \mathbf{y}_q)\}_{q=1}^{Q_\tau} = \{\mathbf{x}_Q, \mathbf{y}_Q\}$ : test portion of downstream dataset  
**Require:** support\_set\_size: size of the support set  $|\mathcal{D}_S^\tau|$   
**Require:** unique()  $\equiv$  function that returns a list of unique classes and list of counts of each class  
**Require:** randint(min, max)  $\equiv$  function that returns a random integer between min and max  
**Require:** choice(range, count)  $\equiv$  function that returns a random list of count integers from range

```
1: procedure SAMPLE_TASK( $\mathcal{D}_{train}, \mathcal{D}_{test}, \text{support\_set\_size}$ )
2:    $\mathcal{D}_S^\tau \leftarrow []$   $\triangleright$  Create an empty list to hold  $\mathcal{D}_S^\tau$ 
3:    $\mathcal{D}_Q^\tau \leftarrow []$   $\triangleright$  Create an empty list to hold  $\mathcal{D}_Q^\tau$ 
4:   train_classes, train_class_counts  $\leftarrow$  unique( $\mathbf{y}_S$ )
5:   test_classes, test_class_counts  $\leftarrow$  unique( $\mathbf{y}_Q$ )
6:   min_way  $\leftarrow$  min(len(train_classes), 5)
7:   max_way  $\leftarrow$  min(len(train_classes), support_set_size)
8:   way  $\leftarrow$  randint(min_way, max_way)  $\triangleright$  Classification way to use for this task
9:   selected_classes  $\leftarrow$  choice(train_classes, way)  $\triangleright$  List of classes to use in this task
10:  balanced_shots = max(round(support_set_size / len(selected_classes)), 1)
11:  max_test_shots  $\leftarrow$  max(1, floor(2000/way))
12:  for all  $c \in$  selected_classes do
13:    class_shots  $\leftarrow$  train_class_counts( $c$ )
14:    shots_to_use  $\leftarrow$  min(class_shots, balanced_shots)
15:    selected_shots  $\leftarrow$  choice(class_shots, shots_to_use)  $\triangleright$  Support shot list
16:     $\mathcal{D}_S^\tau \leftarrow \mathcal{D}_S^\tau + \mathcal{D}_{train}[\text{selected\_shots}]$   $\triangleright$  Add examples to  $\mathcal{D}_S^\tau$ 
17:    class_shots  $\leftarrow$  test_class_counts( $c$ )
18:    shots_to_use  $\leftarrow$  min(class_shots, max_test_shots)
19:    selected_shots  $\leftarrow$  choice(class_shots, shots_to_use)  $\triangleright$  Query shot list
20:     $\mathcal{D}_Q^\tau \leftarrow \mathcal{D}_Q^\tau + \mathcal{D}_{test}[\text{selected\_shots}]$   $\triangleright$  Add examples to  $\mathcal{D}_Q^\tau$ 
21:  end for
22:  return  $\mathcal{D}_S^\tau, \mathcal{D}_Q^\tau$ 
23: end procedure
```

---

which case the images were scaled to  $224 \times 224$  pixels. These hyper-parameters were empirically derived from a small number of runs.

FiT-QDA, FiT-LDA, and FiT-ProtoNets take approximately 12, 10, and 9 hours, respectively, to fine-tune on all 19 VTAB datasets and 5, 3, and 3 hours, respectively, to fine tune all shots on the 4 low-shot datasets.

**BiT** For the BiT few-shot experiments, we used the code supplied by the authors [59] with minor augmentations to read additional datasets. The BiT few-shot experiments were run on a single NVIDIA V100 GPU with 16GB.

For the BiT VTAB-1k experiments, we used the three fine-tuned models for each of the datasets that were provided by the authors [59]. We evaluated all of the models on the respective test splits for each dataset and averaged the results of the three models. The BiT-HyperRule [12] was respected in all runs. These experiments were executed on a single NVIDIA GeForce RTX 3090 with 24GB of memory.

### A.5.2 Personalization on ORBIT Experiments

The personalization experiments were carried out on a single NVIDIA GeForce RTX 3090 with 24GB of memory. It takes approximately 5 hours to train FiT-LDA personalization models for all the ORBIT [5] test tasks. We derived all hyperparameters empirically from a small number of runs. We used the ORBIT codebase<sup>2</sup> in our experiments, only adding the code for splitting test user tasks and slightly modifying the main training loop to make it suitable for FiT training.

---

<sup>2</sup><https://github.com/microsoft/ORBIT-Dataset>

For the personalization experiments, all methods use an EfficientNet-B0 ( $d_b = 1280$ ) as the feature extractor, as it has previously shown superior performance on the ORBIT dataset [28], and an image size of  $224 \times 224$ . FiT-LDA, FineTuner [8] and Simple CNAPs [27] use a backbone pretrained on ImageNet [48], while ProtoNets [23] meta-trained the weights of the feature extractor on Meta-Dataset [10].

The FineTuner [8] results are from [28]. Meta-trained weights for Simple CNAPs [27] and ProtoNets [23] are also taken from [28]. Using these weights, we test these models on the ORBIT test set and report the results.

FiLM layers in FiT-LDA are added to the feature extractor as described in Section 2, resulting in  $|\psi| = 20544$ .

We follow the task sampling protocols described in [5], and train the FiT model for 50 optimization steps using the Adam optimizer with a learning rate of 0.007. The ORBIT test tasks have a slightly different structure in comparison to standard few-shot classification tasks, so in Algorithm A.3 we provide a modified version of data splitting for the classifier head construction. In particular, each test user has a number of objects (classes) they want to recognize, with several videos recorded per object. Each video is split into clips, consecutive 8-frame parts of the video. A user test task is comprised of these clips, randomly sampled from different videos of the user’s objects, and associated labels. Since clips sampled from the same video can be semantically similar, we split the test task so that clips from the same video can only be in either the support or query set, except for the cases when there is only one video of an object available.

---

**Algorithm A.3** Splitting a test task  $\mathcal{D}$  for ORBIT personalization experiments

---

**Require:**  $\mathcal{D}$ : downstream dataset;  $\mathcal{D} = \{\mathcal{D}_c\}_{c=1}^C$ , where  $C$  is the number of classes in test task,  $\mathcal{D}_c$  is data of class  $c$ ;  $\mathcal{D}_c = \{V_{ci}\}_{i=1}^{n_c}$ , where  $n_c$  is the number of videos in class  $c$ ,  $V_{ci}$  is the set of clips from  $i$ th video of class  $c$ ;  $V_{ci} = \{(x_{cij}, c)\}_{j=1}^{n_{ci}}$ , where  $n_{ci}$  is the number of clips in  $i$ th video of class  $c$ ,  $x_{cij}$  is the  $j$ th clip from video  $V_{ci}$

**Require:** batch\_size: size of context split

**Require:** choose( $n, m$ )  $\equiv$  function that randomly samples  $m$  different integers from a set  $\{i\}_{i=1}^n$

**Require:** select\_by\_index( $\mathcal{D}, i$ )  $\equiv$  function that extracts samples of indices  $i$  from a dataset  $\mathcal{D}$

**Require:** diff( $a, b$ )  $\equiv$  function that computes set difference between sets  $a$  and  $b$

**Require:** range( $n$ )  $\equiv$  function that returns a set of values  $\{i\}_{i=1}^n$

```

1: procedure SPLIT_ORBIT_TASK( $\mathcal{D}$ )
2:    $\mathcal{D}_{train} \leftarrow []$ 
3:    $\mathcal{D}_{test} \leftarrow []$ 
4:   num_clips  $\leftarrow$  floor(batch_size/ $C$ )
5:   for  $c \leftarrow 1$  to  $C$  do
6:     num_context_videos  $\leftarrow$  ceil( $n_c/2$ )
7:     context_videos_indices  $\leftarrow$  choose( $n_c$ , num_context_videos)
8:     num_clips_per_video  $\leftarrow$  floor(num_clips/num_context_videos)
9:     if  $n_c = 1$  then
10:      context_clips_indices  $\leftarrow$  choose( $n_{c1}$ , num_clips_per_video)
11:      target_clips_indices  $\leftarrow$  diff(range( $n_{c1}$ ), context_clips_indices)
12:       $\mathcal{D}_{train} \leftarrow \mathcal{D}_{train} +$  select_by_index( $V_{c1}$ , context_clips_indices)
13:       $\mathcal{D}_{test} \leftarrow \mathcal{D}_{test} +$  select_by_index( $V_{c1}$ , target_clips_indices)
14:     else
15:      for  $j \leftarrow$  context_videos_indices do
16:        context_clips_indices  $\leftarrow$  choose( $n_{cj}$ , num_clips_per_video)
17:         $\mathcal{D}_{train} \leftarrow \mathcal{D}_{train} +$  select_by_index( $V_{cj}$ , context_clips_indices)
18:      end for
19:      for  $j \leftarrow$  diff(range( $n_c$ ), context_videos_indices) do
20:         $\mathcal{D}_{test} \leftarrow \mathcal{D}_{test} + V_{cj}$ 
21:      end for
22:     end if
23:   end for
24:   return  $\mathcal{D}_{train}, \mathcal{D}_{test}$ 
25: end procedure

```

---

### A.5.3 Federated Learning Experiments

For each local update a new Adam optimizer is initialized. In each communication round, 5 clients are randomly chosen for making model updates. All of the federated learning experiments were carried out on a single NVIDIA A100 GPU with 80GB of memory. In all experiments we use FiT with the BiT-M-R50x1 [12] backbone pretrained on the ImageNet-21K [16] dataset and ProtoNets head. We derive all hyperparameters empirically from a small number of runs.

**CIFAR100** We train all federated learning models with different number of clients and shots per client for 60 communication rounds. We use a learning rate of 0.003 at the start of the training, decaying it by 0.3 every 20 communication rounds. Upper and lower bound baselines for both the global and personalized scenarios were trained for 400 epochs using the Adam optimizer with a constant learning rate of 0.003. It takes around 20 minutes to train federated learning models, with slightly more training time required for the models with a larger number of shots.

**Quickdraw** We train all federated learning models with a different number of clients and shots per client for 120 communication rounds. We use a constant learning rate of 0.006 for training all federated learning models, except for the model with 50 clients and 2 shots, where we decay the learning rate by 0.3 every 20 communication rounds. Upper bound baseline models, which require training a global model using all available data, were trained for 3000 steps using the Adam optimizer with a constant learning rate of 0.006. Lower baseline models, requiring training a personalized model for each individual, were trained for 400 steps using the Adam optimizer with a learning rate of 0.006. As there are only few samples per class per client, personalized models are trained in a few-shot regime, resulting in overfitting if trained for longer. It takes around 2 hours to train federated learning models, with slightly more training time required for the models with a larger number of shots.